Vanadia Gel Synthesis via Peroxovanadate Precursors. 1. In Situ Laser Raman and ^{51}V NMR Characterization of the Gelation Process

Craig J. Fontenot,[†,‡] Jerzy W. Wiench,[‡] M. Pruski,[‡] and G. L. Schrader*[,†,‡]

Department of Chemical Engineering and Ames Laboratory−USDOE, Iowa State University, Ames, Iowa 50011

Received: June 16, 2000; In Final Form: August 7, 2000

Vanadium oxide gels derived from aqueous solutions of V_2O_5 and H_2O_2 have been investigated using in situ ^{51}V NMR and laser Raman spectroscopic techniques. On the basis of this characterization, a pathway for peroxovanadate decomposition has been proposed, including the presence of two peroxovanadate dimers. New Raman bands and assignments for these species are reported. Gelation was observed to begin both during and after the peroxovanadate decomposition, depending on the initial molar ratios of H_2O_2/V and the total concentration of vanadium. Experimental ^{51}V NMR evidence suggested that the VO_2^+ species was directly involved in the formation of the gel.

1. Introduction

Transition metal oxides such as MoO_3, WO_3, TiO_2, and V_2O_5 can be prepared by the dissolution of metals, metal oxides, or metal salts into aqueous solutions of H_2O_2.[1−3] V_2O_5 materials prepared by this chemistry have important electronic and ionic properties utilized in antistatic coatings, battery cathodes, and electrical components. Extensive work has been performed on the convenient synthesis of V_2O_5 gels from H_2O_2 and $NaVO_3$, including a process involving ion exchange.[4,5] More recently, the preparation of materials ($V_2O_5 \cdot nH_2O$) by a sol−gel procedure utilizing V_2O_5 has also been reported.[6] Peroxovanadates derived from V_2O_5 are attractive precursors to vanadia gels in that they are inexpensive and fairly easy to handle. Gel formation occurs quite readily, but as for alkoxide sol−gel preparation routes, the reactivity of the precursor solutions depends on pH, temperature, and reactant concentrations.

Our interest in peroxovanadates is based on their use for catalyst synthesis via sol−gel chemistry.[7,8] Using this route, we have been able to prepare a wide range of mixed metal oxide catalysts that are active for reactions such as the selective oxidation of 1,3-butadiene. Brazdil et al. have described the preparation of vanadium−antimony oxide catalysts for the selective oxidation or ammoxidation of several hydrocarbons.[9,10] The advantages of these materials were increased catalytic activity, milder preparation conditions, homogeneous distribution of the metal constituents, increased surface area and porosity, and resistance to attrition.[11] These improvements were attributed to the microcrystalline nature of the catalyst resulting from thermal treatment of the sol−gel material. The driving force for the preparation of these catalysts was thought to be a redox reaction between the V^{5+} peroxo complex and Sb^{3+} (Sb_2O_3) which formed a vanadium antimonate xerogel comprised of V^{4+} and Sb^{5+}. These researchers also suggested that additional characterization of the sol−gel chemistry and the reaction mechanisms would be desirable, especially using in situ spectroscopic techniques.

Characterization of reacting species during formation of a gel is challenging, and only a few techniques are likely to be applicable and informative under in situ conditions. Both laser Raman and NMR spectroscopies have been previously used by our research group for in situ characterization of catalysts. Prior research has indicated that formation of several vanadium peroxo complexes is likely and that interconversion may be relatively easy. The reaction of metavanadate salts and H_2O_2 in aqueous solutions has been characterized by Raman,[12−15] ^{51}V NMR,[16−19] ^{17}O NMR,[18] and UV−visible spectroscopy.[9,20] Most of the recent literature is in general agreement regarding the identification of these species, although some discrepancies still exist regarding the structure of the complexes and the spectral assignments. Some researchers have directly related characterization of the precursor species to V_2O_5 gel formation. The condensation of vanadates from a metavanadate precursor was studied by Pozarnsky and McCormick.[4,5] An ion-exchange column was used to obtain an acidic solution containing the dioxovanadate cation and protonated forms of the decavanadate anion. Using ^{51}V and ^{17}O NMR to follow the reaction, these researchers reported that the dioxovanadate cation was involved with the initiation of condensation. The $V_2O_5-H_2O_2$ preparation route may be expected to behave similarly to the $NaVO_3-H_2O_2$ method, and further characterization utilizing ^{51}V NMR spectroscopy has been performed by Alonso and Livage.[6] These researchers demonstrated that dissolution of the oxide led to the formation of unstable diperoxo $[VO(O_2)_2]^-$ species which decomposed to form a monoperoxo species $[VO(O_2)]^+$. Vanadate and decavanadic acid entities were then produced before polymerization formed $V_2O_5 \cdot nH_2O$.

The research performed in our studies has focused on the combined use of laser Raman and ^{51}V NMR to elucidate the sol−gel chemistry relevant to the preparation of active, selective, and stable selective oxidation catalysts involving V_2O_5 and other components. A summary of the spectral assignments for the laser Raman and NMR characterization will be provided, and three in situ spectroscopic studies will be presented for representative materials prepared by procedures relevant to our preparations of V_2O_5-based catalysts. More extensive characterization of the final solid-state material and the results of catalytic studies will be reported in other publications.[7,8]

* To whom correspondence should be addressed.
[†] Department of Chemical Engineering.
[‡] Ames Laboratory−USDOE.

10.1021/jp0021897 CCC: $19.00
Published on Web 11/17/2000

TABLE 1: Summary of Samples

sample	C_V	temp (°C)	$n(H_2O_2)$:n(V)	initial pH	final pH	pH adjusted	solid formed	surface area (m^2/g)
A	0.11	25	7.9	0.95	1.47	0.58 mL of HCl	red viscous sol	1−2
B	0.11	25	7.9	1.28	2.31	n/a	red viscous sol	1−2
C	0.50	5	25	0.80	n/a	n/a	brown gel	1−2

TABLE 2: Laser Raman and ^{51}V NMR Characterization of Species Observed in Peroxovanadate Solutions[a]

species			Raman shift (cm^{-1})	Raman refs	^{51}V NMR shifts (ppm)	NMR refs	obsd in sample
1	monperoxovanadate cation	$VO(O_2)(OH_2)_3^+$	977, 891, 542, 314 [977, 890, 540, 320]	12, 23, 24	−541 [−540]	17	A−C
2	diperoxovanadate anion	$VO(O_2)_2(OH_2)$	985, 891, 633, 537 314 [985, 890, 640, 540 320]	12, 23, 24	−695 (−711) [−692]	17	A−C
3	protonated diperoxovanadate	$HVO(O_2)_2(OH_2)$			−705 (−720) [−702]	17	A
4	symmetric dimer	$[VO(O_2)_2]_2O(H_2O)_2$	960, 910, 864, 598	this work	−670 [−670]	16	A, B
5	asymmetric dimer	$H_4[(O_2)_2OVOVO_2(O_2)]$	955, 910, 599, 490, 410	this work	−669, −674 [−670.6, −674]	18	C
6	diprotonated decavanadate ion	$H_2V_{10}O_{28}^{4-}$	1007, 980, 935, 836, 547, 314 [1005, 981, 935, 850, 595, 550, 450, 320]	33	−426 to −428 (−426) [−426] −512 to −513 (−509) [−512] −531 to −533 (−532) [−531]	4	A−C
7	dioxovanadium cation	VO^{2+}	940 [940, 910]	14	−545 [−545]	16	A−C
8		?			−641		A,C

[a] Values in parentheses were obtained at 5 °C; those in square brackets are from previous literature.

2. Experimental Section

2.1. Sample Preparation. Preparation conditions for the V_2O_5 gels are summarized in Table 1 (samples A−C). Solutions of 0.1 M peroxovanadate were prepared by addition of 30% H_2O_2 (Fisher Chemicals) to slurries of deionized water and V_2O_5 (Alpha Aesar). Solutions of 0.5 M peroxovanadate were prepared by addition of V_2O_5 to H_2O_2. Temperatures were controlled using a Brinkmann Instruments circulating liquid bath. Samples A and B were maintained at 25 °C. Preparations at high concentrations of V_2O_5 or H_2O_2 at 25 °C were completed within a minute; thus for sample C, the temperature was reduced to 5 ± 1 °C in order to perform the in situ characterization studies.

2.2. Characterization. *2.2.1. Laser Raman Spectroscopy.* Laser Raman spectra were obtained using Coherent 532-50 diode-pumped laser (532 nm, 50 mW at the source) and were collected at 180° using a Kaiser probe head coupled via fiber optics to a Kaiser Holospec *f*/1.8 spectrometer. For Raman characterization, the temperature was controlled using a water-jacketed in situ flow cell. For high concentrations of vanadium (>0.5 M), laser-induced decomposition was observed at room temperature, as reported by other researchers. To avoid sample decomposition, a Bruker RFS-200 FT Raman spectrometer (1024 nm, 50 mW at the source) was used to confirm spectral assignments. Liquid samples were also spun to reduce sample heating and decomposition.

2.2.2. ^{51}V Nuclear Magnetic Resonance. ^{51}V NMR spectroscopy was performed at 9.4 T using a Chemagnetics Infinity spectrometer operated at 105.17 MHz. Liquid samples were placed in glass tubes for use with a standard Chemagnetics 5 mm probe. Measurements were performed at temperatures between 5 and 25 °C (± 0.5 °C). Typically, 30−120 spectra were obtained during the sol−gel processes, in some cases involving up to 140 h. Due to fast longitudinal relaxation, a delay of only 50 ms between scans was needed to record fully equilibrated magnetization. Approximately 720 scans were collected to produce an intense ^{51}V signal. Liquid spectra exhibited narrow resonances that could be assigned to various reaction products and intermediates. The concentrations of various species were determined using deconvolution and integration software available from Spinsight. The liquid-state spectra reported in this work did not include the V^{4+} species, which are paramagnetic. In addition, the solid products "dropped out of sight" as they condensed at the bottom of the NMR tube, outside of the coil. Even if they remained in the coil, however, they would not be observable in the static NMR experiments due to the chemical shift anisotropy and quadrupolar broadening. A detailed solid-state NMR analysis of the solid products of our synthesis is described elsewhere.[21] All spectra are reported with reference to vanadium oxytrichloride ($VOCl_3$), using the δ scale with negative values being upfield.

2.2.3. pH Measurements. All pH measurements were taken using an Orion Model 410A meter and an Orion Ross Sure-Flow glass body electrode.

3. Results

3.1. Characterization of Species Observed in Peroxovanadate Solutions. The vanadate species observed in our experiments and their corresponding Raman and ^{51}V NMR assignments are summarized in Table 2.[4,12,14,16−18,23,24,33] To facilitate the subsequent discussion, these species are identified in boldface numerics. New Raman bands and assignments are reported for two diperoxovanadate dimers. A brief discussion of the previous Raman characterization of monomer peroxovanadates is useful in understanding these new results.

Both the mono- (**1**) and diperoxo (**2**) complexes have been reported to be fairly stable within specific pH domains, although the monoperoxo cation has been observed to be a better oxidant than the diperoxo anion.[22] Laser Raman spectra of **1** and **2** have been previously reported.[12,23,24] For our studies, the V═O stretches for these species were observed at about 977 and 985 cm^{-1} respectively; the δ(V═O) deformations were observed at about 314 cm^{-1}, consistent with other studies.[23,24] The bidentate peroxide ligand has local C_{2v} symmetry resulting in three IR and Raman active modes: the O_p–O_p stretch, the symmetric ν^1(V−O_p) stretch, and the asymmetric ν^3(V−O_p) stretch. For **1**, the coordination is symmetric, and the symmetric and asymmetric stretches [ν^s(V−O_p) and ν^{as}(V−O_p)] overlap at ∼540 cm^{-1}. Diperoxo complexes can have pentagonal pyramidal or pentagonal bipyramidal coordination (**2** and **3**).[24] For **2**, the presence of the additional bidentate peroxo ligand (in addition to the coordinated water molecule) increases the bond length of V−O_{cis} relative to V−O_{trans} (Figure 1), where O_{cis} and O_{trans} denote the oxygen atoms adjacent to or across from

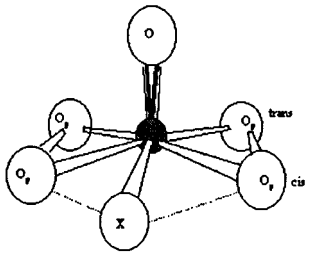

Figure 1. Pentagonal pyramidal structure of diperoxovanadate anion, where X is H_2O.

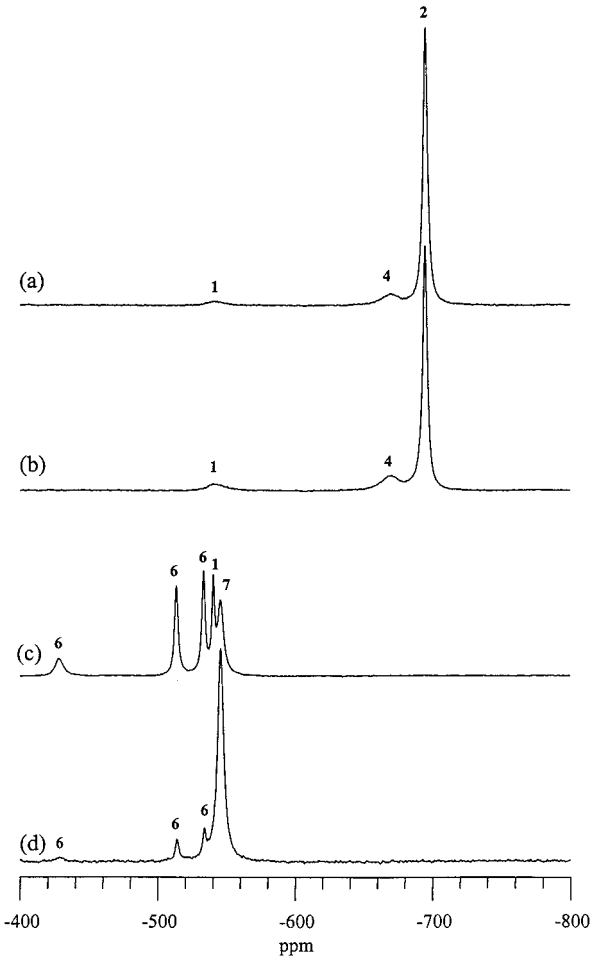

Figure 2. ^{51}V Solution NMR of sample A at (a) 20, (b) 40, (c) 158, and (d) 1800 min.

the coordinated water ligand. This asymmetry results in a splitting of the symmetric and asymmetric $V-O_p$ bands,[15] so that the symmetric $\nu^1(V-O_p)$ band was observed at about 633 cm^{-1} and the asymmetric $\nu^3(V-O_p)$ band was observed at about 542 cm^{-1}. Although the O_p-O_p bond in **2** is longer than in **1**, there was no distinguishable difference in the position of the observed band.[15] It should also be noted that for an unidentate, end-on coordinated hydroperoxide, only one $V-O_p$ stretch would be observed, and an OOH deformation should be observed above 1100 cm^{-1}.[25]

In our studies we detected Raman bands for a symmetric diperoxovanadate dimer (**4**) and an asymmetric peroxo dimer (**5**). Bands at 960, 910, and 598 cm^{-1} were assigned to **4**, which probably corresponded to $V-O_b-V$, O_p-O_p, and the $V-O_p$ vibrations, respectively. Since the $V-O_b-V$ stretch was observed at rather high wavenumbers (close to the V═O stretch at ∼995 cm^{-1}) instead of at lower wavenumbers where the bent V_2O bands might be expected, a linear μ_2-bridging oxygen ligand

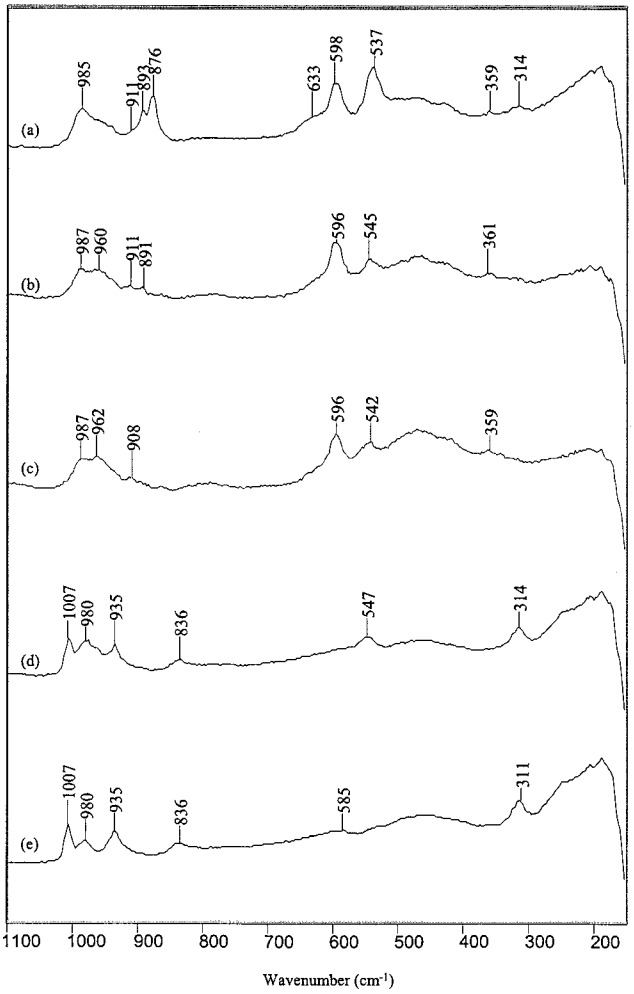

Figure 3. Laser Raman spectra of sample A at (a) 20, (b) 40, (c) 60, (d) 158, and (e) 1240 min.

(O_b) having some π character was likely present. The absence of splitting of the symmetric and asymmetric $V-O_p$ stretches was consistent with the lack of H_2O coordination in the same plane as the η^2-peroxo ligands. Therefore, the local structure around the vanadium was octahedral, not pentagonal bipyramidal. Bands at 955, 910, and 599 cm^{-1} and in the 400 and 500 cm^{-1} regions were assigned to the asymmetric dimer, **5**. The bands at 955, 910, 599 cm^{-1} were analogous to the symmetrical dimer, while the bands from 400 to 500 cm^{-1} were assigned to V−OH stretches.

3.2. Characterization of Vanadia Gel Formation. The LRS and ^{51}V NMR results correlated quite well, although some subtle differences were apparent with respect to time. However, the differences generally did not extend over time periods greater than 1 min.

SAMPLE A. ^{51}V NMR at 20 min (after peroxide addition) revealed that **2** was predominant (Figure 2a). Also present (in order of decreasing signal intensity) were **4**, **1**, and **3** (low intensity). Raman data (Figure 3a) acquired at this time revealed a very strong band at 537 cm^{-1} which was assigned to **1** and **2**. The strong band at 598 cm^{-1} was assigned to **4**, while the sharp band at 876 cm^{-1} was assigned to the $\nu(O_p-O_p)$ stretch of H_2O_2. A broad band between 1023 and 930 cm^{-1} was assigned to the superposition of the V═O stretch for **2** (990 cm^{-1}), **1** (977 cm^{-1}), and **3** (present in a low concentration). Sharp bands at 893 and 314 cm^{-1} were assigned to **1** and **2**.

At 40 min, Raman bands emerged at 960 and 911 cm^{-1} (Figure 3b); these features persisted until 68 min. The Raman

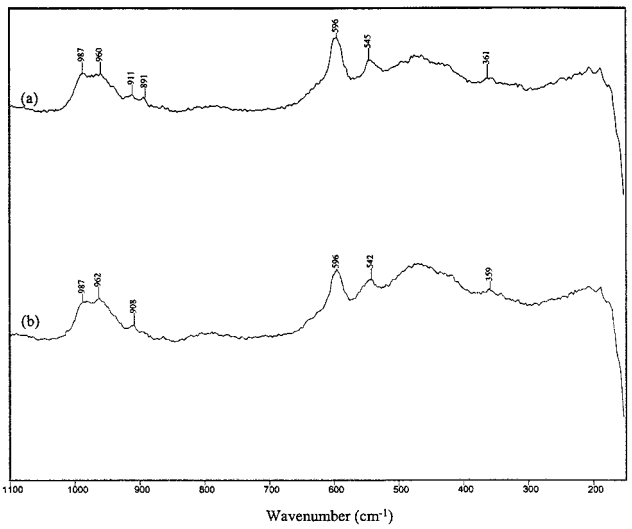

Figure 4. Laser Raman spectra of sample A (when dimer was at a maximum) at (a) 40 and (b) 60 min.

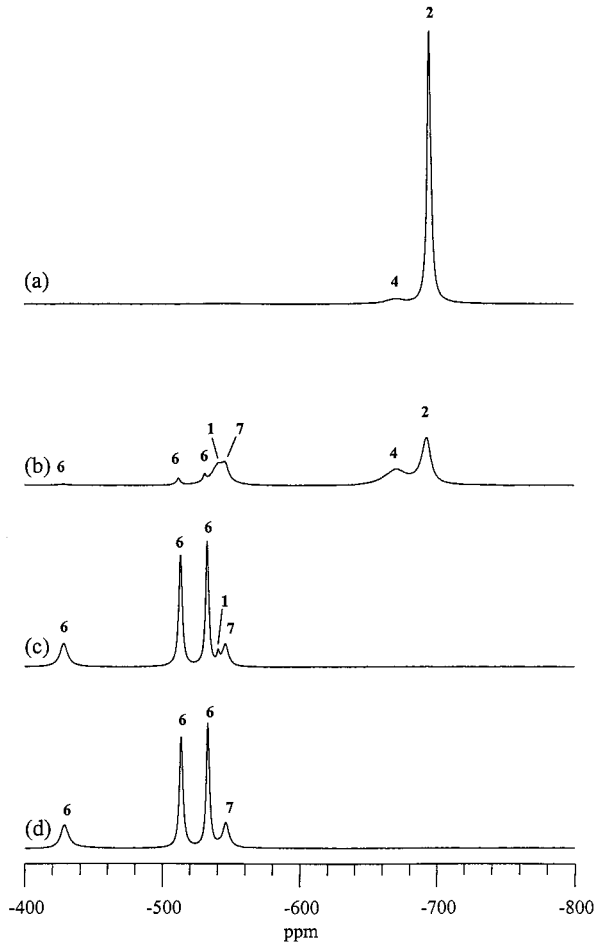

Figure 5. [51] V Solution NMR of sample B at (a) 7, (b) 68, (c) 268, and (d) 1000 min.

bands were the most intense from 40 to 60 min (Figure 4a,b). [51]V NMR revealed that **1**, **2**, and **4** (Figure 2b) were present at this time, with **4** being at maximum concentration. Raman bands were assigned to **1** and **2** on the basis of previous work.[12] The Raman bands at 911 and 596 cm^{-1} were assigned to **4**. As time progressed, the band corresponding to the $O_p–O_p$ stretch (876 cm^{-1}) due to H_2O_2 decreased in intensity, until its intensity was very low at 68 min. A decrease in the concentration of **2** coincided with the complete consumption of H_2O_2.

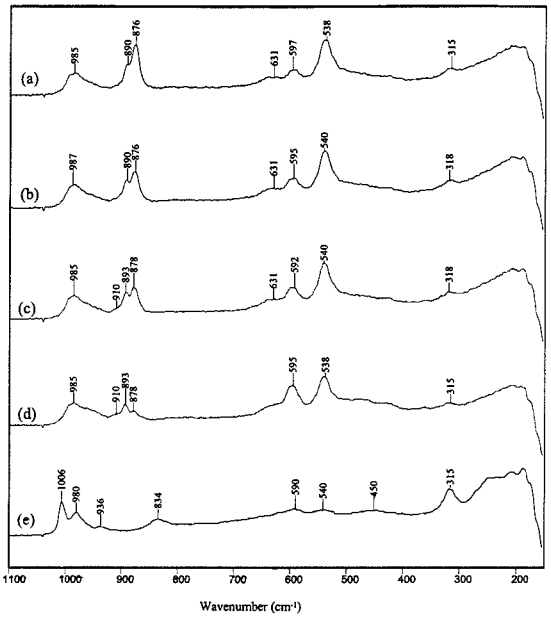

Figure 6. Laser Raman spectra of sample B at (a) 7, (b) 55, (c) 60, (d) 70, and (e) 268 min.

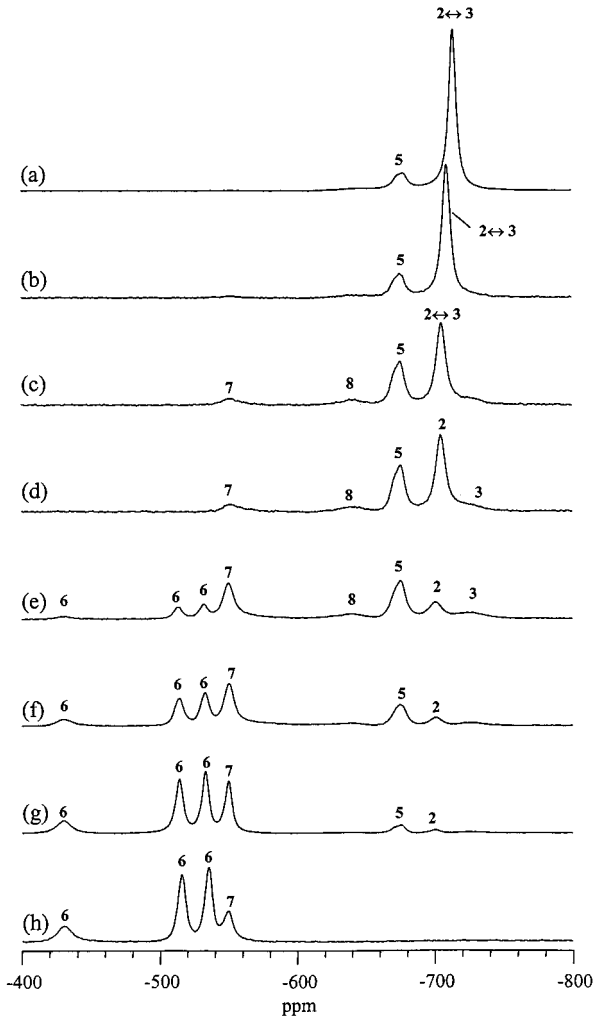

Figure 7. [51] V Solution NMR of sample C at (a) 5, (b) 174, (c) 341, (d) 393, (e) 415, (f) 485, (g) 614, and (h) 1011 min.

At 158 min, [51]V NMR characterization revealed the presence of **6**, while **4** had nearly disappeared (Figure 2c). Raman acquired at this time (Figure 3c) showed bands characteristic

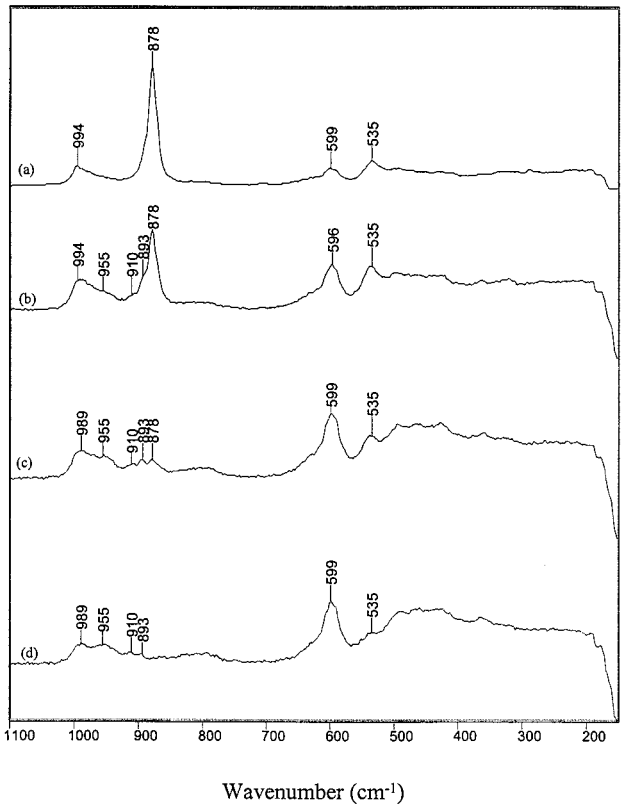

Figure 8. Laser Raman spectra of sample C taken at time (a) 5, (b) 174, (c) 341, and (d) 393 min.

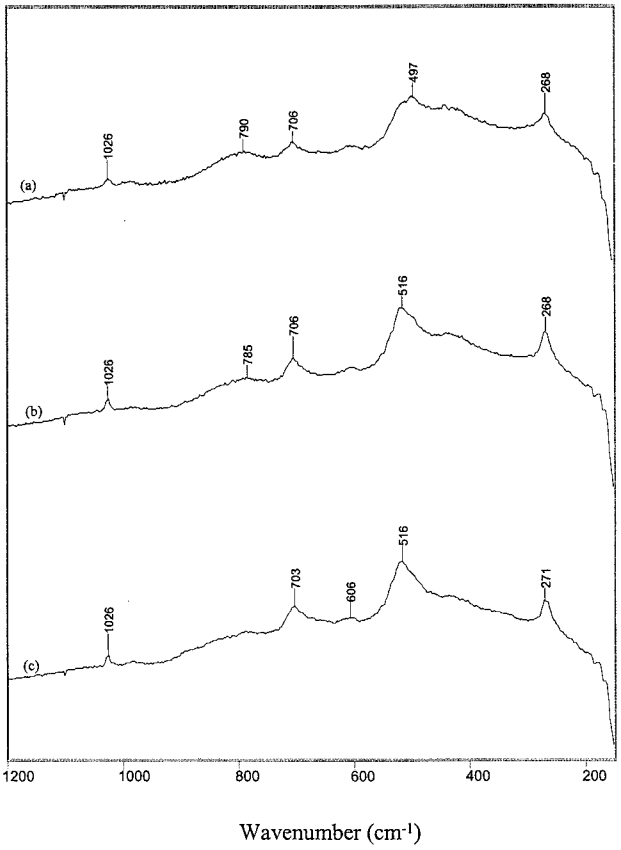

Figure 9. Laser Raman spectra of sample C taken at time (a) 415, (b) 485, and (c) 1523 min.

of **6**. The band at 936 cm^{-1} could also be assigned to **7**, but another band at 910 cm^{-1} would also be expected.[14] By 1240 min (Figure 3d), bands corresponding to **6** had become more distinct, but little change was observed in the Raman characterization after this time.

At $t > 200$ min, only **1, 6**, and **7** were present in solution, as clearly revealed by ^{51}V NMR spectroscopy. The concentrations of **6** and **7** increased as **1** disappeared (this transformation was nearly complete at about 1400 min). At this point, the peaks due to **6** and **7** began to decrease in intensity, coinciding with the initial sol−gel formation (Figure 2d).

SAMPLE B. At 7 min (pH =1.42), the solution was clear and red. ^{51}V NMR revealed that **2** was the predominant species. Also observed (in order of decreasing signal intensity; see Figure 5a) were **4**, **1**, and **7**. The Raman spectrum (Figure 6a) at this time showed a sharp band at 876 cm−1 for H_2O_2. Another strong band observed at 538 cm^{-1} corresponded to **2**. The broad band observed between 1000 and about 960 cm^{-1} involved an overlap of bands for **2** and **4**. A sharp band began to become distinguishable at 890 cm^{-1} and was assigned to **1** and **2**. The band at 597 cm^{-1} was assigned to **4**, while the band at ∼315 cm^{-1} was due to **1** and **2** (although **1** was again present in low concentration). A broad shoulder was also observed at 631 cm^{-1} and was assigned to **2**.

The ^{51}V NMR spectra obtained between 55 and 80 min revealed interesting transformations: peaks assigned to **2** decreased in intensity, while those for **4** increased to a maximum at ∼68 min (Figure 5b) and then decreased. Meanwhile, **6** appeared at 60 min and increased in concentration. The pH changed substantially in this time domain from ∼1.5 at 55 min to ∼2.2 at 80 min. The Raman spectra taken at 55 min (Figure 6b) and 60 min (Figure 6c) showed **4** at maximum concentration. As the reaction proceeded, there was a further decrease in intensity of the H_2O_2 band at 876 cm^{-1}, compared to bands for **1** and **2**. At about 70 min this Raman band had nearly disappeared, indicating that H_2O_2 was eliminated (Figure 6d). As for sample A, there was a concomitant decrease in the concentration of **2**. The pH of the solution at this time was 1.45, and without excess H_2O_2, **1** rather than **2** would be expected to be the dominant species[17,18]

At 268 min and pH = 2.45, the solution was clear and dark red. The Raman spectrum revealed bands corresponding to **6**. The ^{51}V NMR spectrum showed that species **1** and **7** were also present (Figure 5c). The Raman spectra did not change significantly at later times.

After 1000 min, the ^{51}V NMR spectrum (Figure 5d) again had peaks corresponding to **6** and **7**. At 1600 min, the total vanadium concentration in solution began to decrease, likely corresponding to the formation of a solid.

SAMPLE C. At 5 min, a ^{51}V NMR peak was observed at −714 ppm. This was assigned to **2** in the limit of fast proton exchange with **3** (denoted 2↔3), so that only one peak was observed. Also observed were **5** and an unknown species **8** (Figure 7a). The Raman spectrum at this time (Figure 8a) showed a very strong band at 878 cm^{-1}. This band likely involved both H_2O_2 (878 cm^{-1}) and **2** (890 cm^{-1}) and also possibly involved an overlap with a shoulder at 910 cm^{-1} perhaps due to **5**. Excess peroxide produced such a large Raman band intensity that the other bands in this region were not discernible. A very broad peak observed in the range from 1015 to 930 cm^{-1} with a maximum at about 994 cm^{-1} resulted from a superposition of several bands involving **2** (990 cm^{-1}) and probably the $V-O_b-V$ stretch of **5** (∼955 cm^{-1}). The band at 599 cm^{-1} was assigned to **5** [probably $\nu(V-O_p)$]. The sharp band at 535 cm^{-1} corresponded to the 2↔3 assignment.

By 174 min, the Raman shoulder bands at both 955 and 910 cm^{-1} appeared more pronounced. Also, a broad Raman band

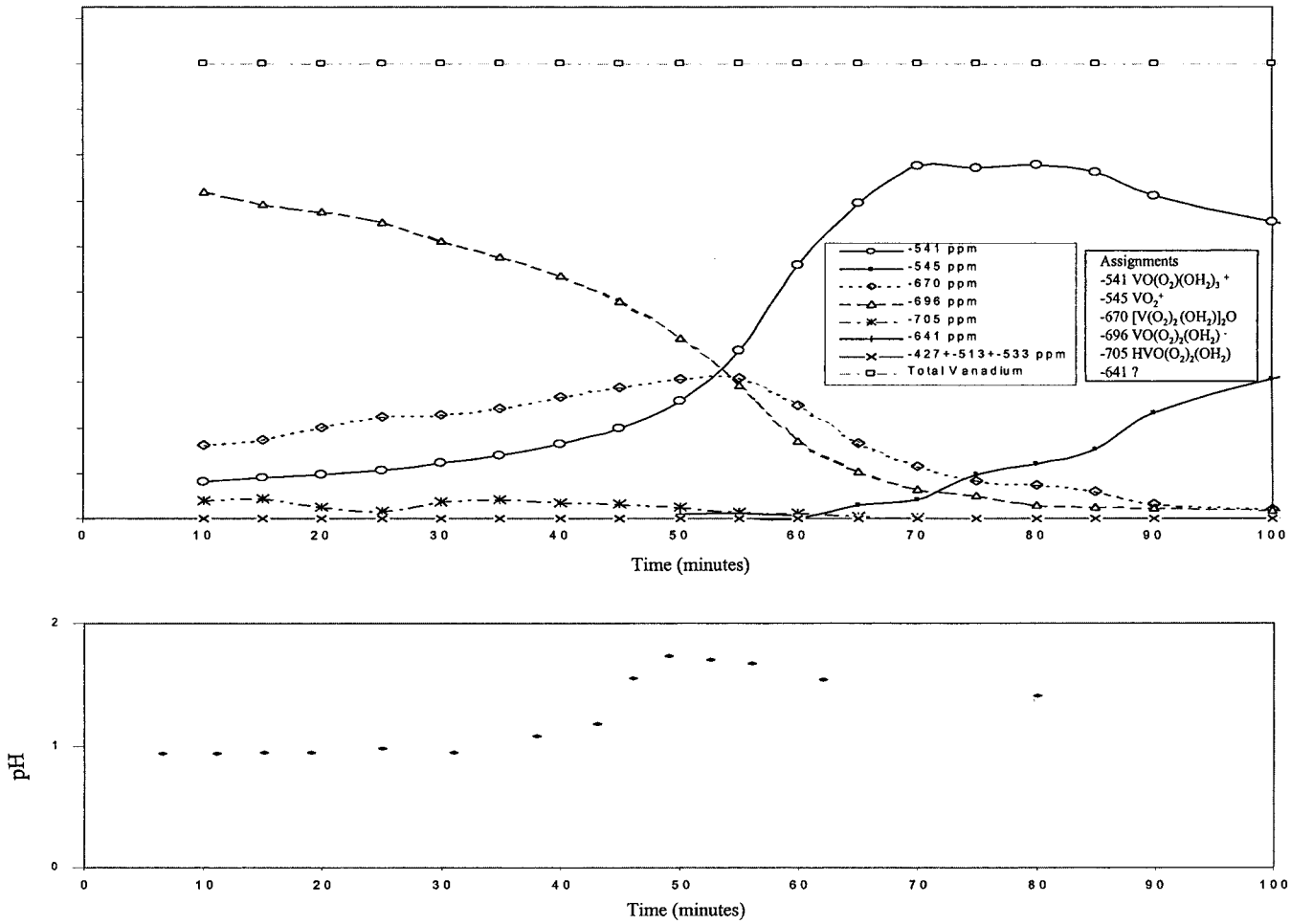

Figure 10. ^{51}V NMR and pH vs time for sample A.

was observed between 478 and 423 cm^{-1} and was attributed to V−OH stretches for **5** (Figure 8b). This observation correlated with the ^{51}V NMR results, which showed that the signals due to **5** had increased (Figure 7b). The ^{51}V peak for **2**↔**3** began to separate and shift downfield. Since the peak for **2**↔**3** represents the center of mass for **2** and **3** (in the limit of fast exchange), this shift is probably due to the change in relative concentrations of these species, in this case, an increase in **2** relative to **3**. Raman spectra at $t > 174$ min were difficult to obtain due to the extremely dark color of the solution.

At 393 min, ^{51}V NMR signals for **5** and **7** had increased, with **5** at its maximum (Figure 7d). The signal for **2**↔**3** continued to shift and separate, likely indicating that the rate of proton transfer between **2** and **3** had decreased. Raman spectra were difficult to obtain due to the darkening of the solution. At that time, Raman bands corresponded to **5** (955, 910, 599, 410−490 cm^{-1}) and **2** (989, 893, 535 cm^{-1}). The band at 878 cm^{-1} was absent, indicating that H_2O_2 was no longer present (Figure 8d).

At 415 min, the ^{51}V NMR spectrum indicated that **5** had become the predominant species in solution. The signal for **2**↔**3** had decreased in intensity, and a broad but distinguishable signal corresponding to **3** had appeared (Figure 7e). At this time, the solution had become dark red and was sufficiently viscous to effectively trap small O_2 bubbles evolved from the solution. Although Raman data became even more difficult to obtain due to the color of the sample, bands could be observed at 1026, 706, 497, and 268 cm^{-1} (Figure 9a). Since ^{51}V NMR does not reveal the presence of any new species, the band at 1026 cm^{-1} might be due to the V═O stretch of a short polymeric segment. This band might also be attributed to **8**, although the concentration would be very low.

At 485 min, ^{51}V NMR showed that the signals for **7** had increased, while the ones due to **2** and **3** were completely separated and had decreased in intensity. The concentration of **6** was relatively unchanged (Figure 7f). Again, the solution was very dark and viscous. Raman bands were observed (Figure 9b) at 1026, 706, 516, and 268 cm^{-1}. The viscosity continued to increase; this increase leads us to believe that the band at 1026 cm^{-1} was the V═O stretch of a short polymer segment.

At 614 min, ^{51}V NMR showed that the concentration of **6** had increased at the expense of **2** and **5** (Figure 7g). The total amount of vanadium in solution began to decrease indicating that formation of a solid had begun. By 1011 min, a gel was present and only **6** and **7** were found in solution (Figure 7h). By 1523 min, the reaction was nearly complete, and a solid had formed. The Raman spectrum of this wet gel had strong bands at 703, 516, and 271 cm^{-1}. The weak band at 1026 cm^{-1}, previously observed at 485 min, was also present (Figure 9c).

4. Discussion

4.1. Solution Chemistry. Preparation conditions for samples A and B ($C_V = 0.1$ M, $H_2O_2/V = 7.9$) were similar, except for the pH: for sample A, the pH was lowered using HCl, while the pH of sample B was unadjusted. The same vanadate species were identifiable for these synthesis conditions, although the time of observation and the relative concentrations of the

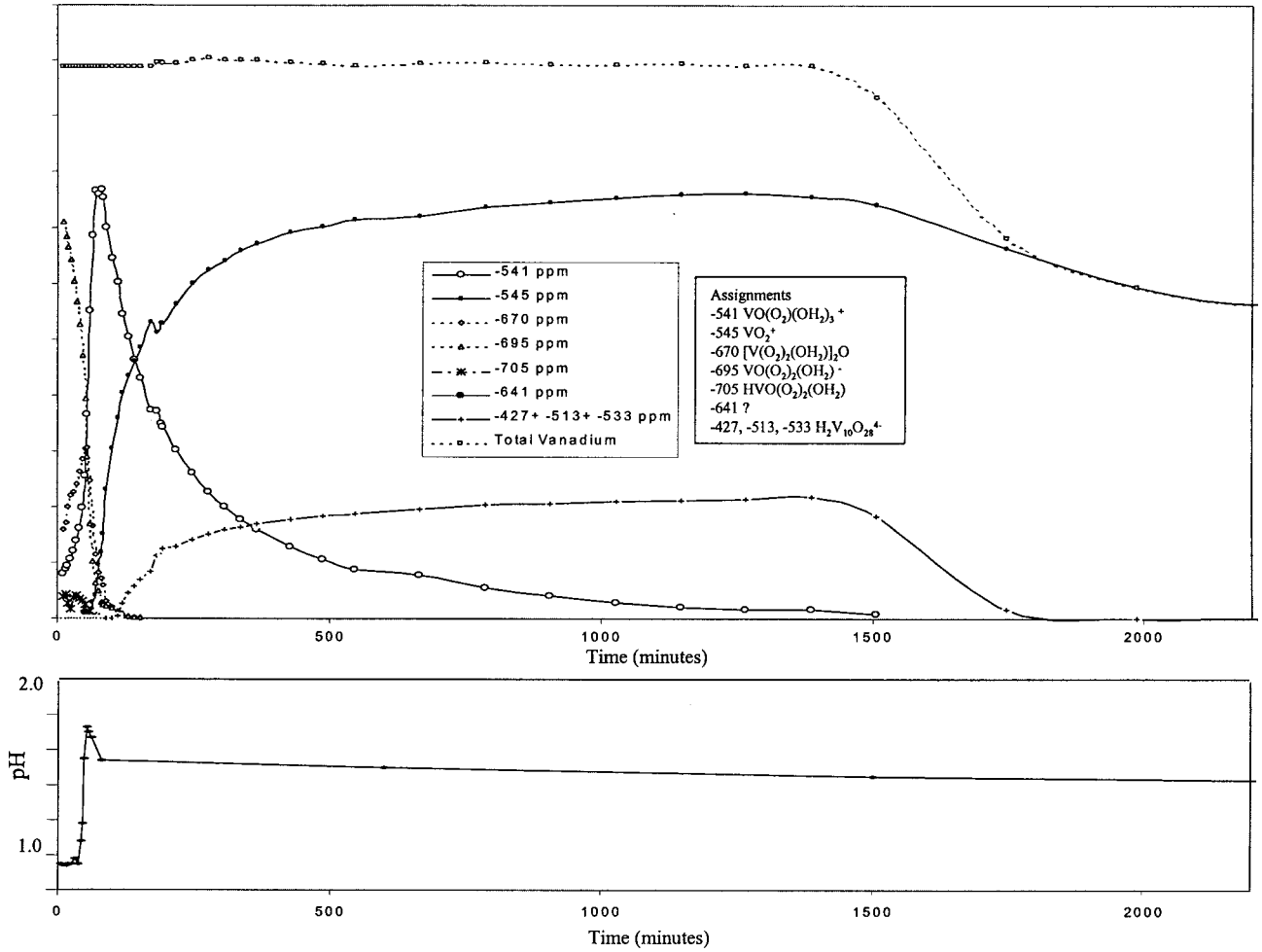

Figure 11. ^{51}V solution NMR vs time and pH vs time for sample A.

complexes differed (Figures 10−13). The only exception was the protonated diperoxovanadate species, observed only in samples A and C. A plausible conversion pathway is given below:

$$V_2O_5 + 2H^+ + 2H_2O_2 + 3H_2O \rightarrow 2VO(O_2)(OH_2)_3^+ \quad (1)$$

$$VO(O_2)(OH_2)_3^+ + H_2O_2 \leftrightarrow VO(O_2)_2(OH_2)^- + 2H^+ + 2H_2O \quad (2)$$

$$2VO(O_2)_2(OH_2)^- + 2H^+ \rightarrow [V(O_2)_2(OH_2)]_2O^\circ + H_2O \quad (3)$$

$$[V(O_2)_2(OH_2)]_2O^\circ + 3H_2O + 2H^+ \rightarrow 2VO(O_2)(OH_2)_3^+ + O_2 \quad (4)$$

$$2VO(O_2)_2(OH_2)_3^+ \rightarrow 2VO_2^+ + O_2 + 6H_2O \quad (5)$$

$$10VO_2^+ + 8H_2O \leftrightarrow H_2V_{10}O_{28}^{4-} + 14H^+ \quad (6)$$

$$VO_2^+ \rightarrow \text{solid} \quad (7)$$

The diperoxovanadate anion was the predominant peroxo species in solution initially. However, the decomposition of the peroxo complexes was thought to occur primarily through reactions 4 and 5 involving the monoperoxo and dimer species. This is in partial agreement with a previous study,[19] which reported that the most likely pathway of the η^2-peroxo ligand species was by decomposition of the monoperoxovandate cation. The role of the dimer has not been clearly established previously, and in our studies this major intermediate introduces a new pathway for peroxo decomposition. In another recent study[6] (molar ratio of $H_2O_2/V = 29.4$), an increase in peroxide concentration was observed to have the following effects: (1) the monoperoxovanadate cation was a predominant species in solution; (2) the diperoxovandate anion was stable for longer times; (3) the dimer was only observed in trace amounts; and (4) the gel formed rapidly. An increase in the H_2O_2/V ratio would initially favor the formation of more monomer peroxo species than dimer peroxo species. A higher concentration of peroxide would also result in a lower pH through reaction 2, and therefore the monoperoxo species would be expected to dominate after the excess H_2O_2 had been consumed.

The consistency of the proposed chemistry and the trends in pH are most easily confirmed for sample A since the species evolved in a sequential manner. The Raman spectra showed that H_2O_2 was present until about 40 min, so reaction 2 continued until this time. The cycle, monoperoxo→diperoxo→dimer→monoperoxo (reactions 2−4) continued as long as excess peroxide was available. The pH remained constant during this cycle, which indicated that in the absence of other reactions the rate of reaction 2 equaled the sum of the rates of reactions 3 and 4. Once the excess peroxide had been consumed, reaction 2 ceased (H^+ was no longer produced), and reaction 5 proceeded. Reactions 3 and 4 still occurred, although now without reaction 2 occurring the pH was observed to increase.

In samples A and B, all of the peroxo complexes eventually

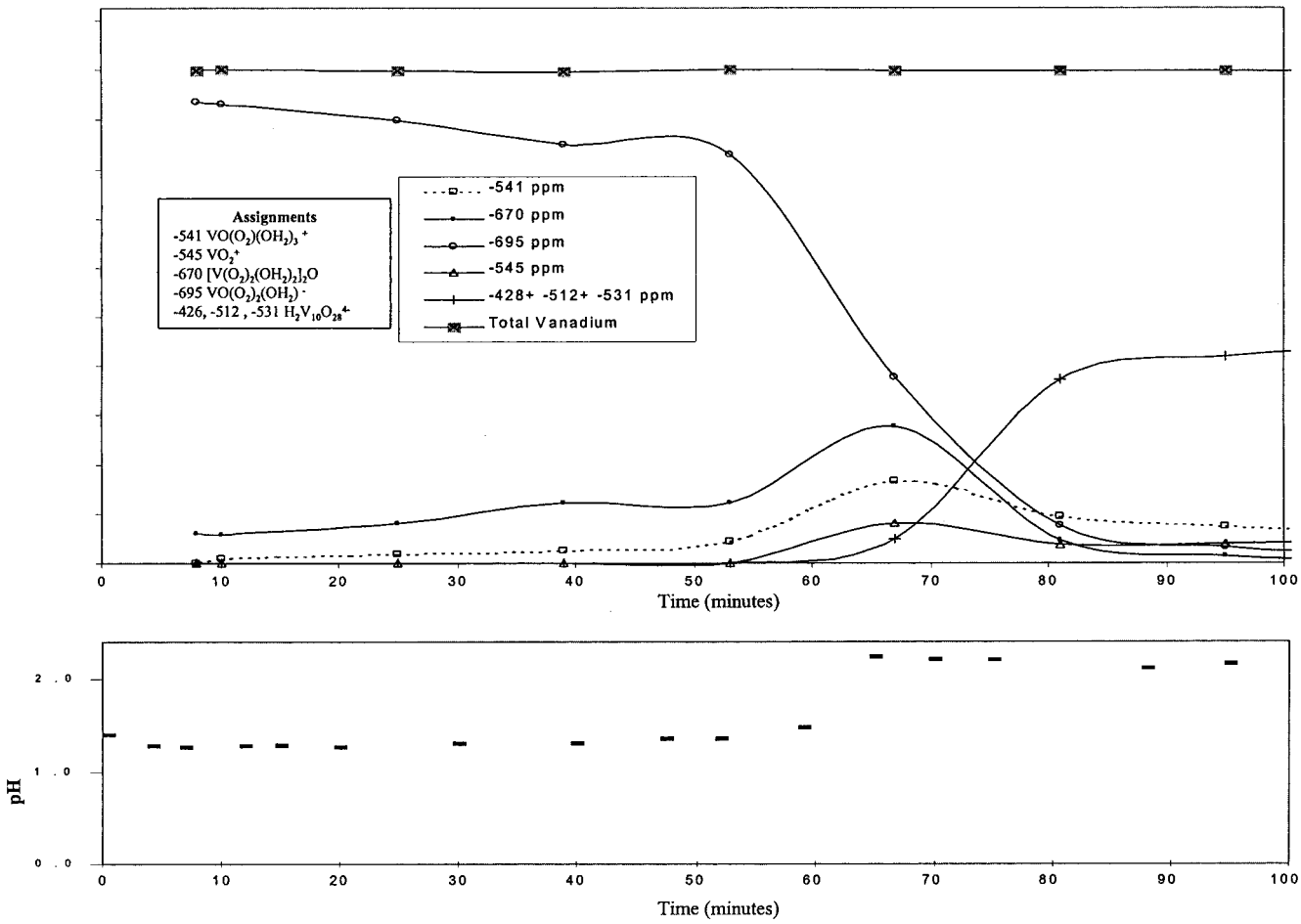

Figure 12. ^{51}V NMR and pH vs time for sample B.

decomposed, and at long times (>150 min), only the diprotonated decavanadate anion, the dioxovanadium cation, and the monoperoxovanadate cation were detected. The relative concentrations of the first two species remained relatively constant until the monoperoxovanadate cation had disappeared. The protonated diperoxovanadate complex existed only in the presence of excess H_2O_2 and in highly acidic solutions (pH < 1). As the monoperoxovanadate cation disappeared, the overall vanadium concentration in solution as detected by ^{51}V NMR began to decrease, indicating that the polymerization process had begun. For sample A, polymerization began at about 1700 min and proceeded rapidly until the decavanadate ion was depleted (Figure 11). In sample B, the same trends were observed, although the decavavanadate ion was not depleted (Figure 13). In both samples A and B, the decavanadate ion acted as the source of vanadium in solution (reverse of reaction 6).

4.2. Gelation. Gelation occurred only in the presence of the VO_2^+ cation (i.e. samples A−C) and probably proceeded via a mechanism similar to those reported by other authors,[4,26] with the VO_2^+ cation being directly involved. However, samples A−C yielded solids different than those previously reported, as will be discussed in the second part of this study. The condensation/gelation processes that occurred in samples A and B were believed to occur as the VO_2^+ cation or a reactive intermediate[4,26] reacted through oxolation to form chains. The exact precursor for polymerization is still unclear, but involvement of the VO_2^+ species is strongly indicated. Livage et al.[26] have stated that the neutral $VO(OH_3)$ species is the reactive precursor. $VO(OH)_3$ has been reported[27] to be formed via the hydroloysis of VO_2^+ as

$$VO_2^+ + 2H_2O \leftrightarrow H^+ + VO(OH)_3°(aq)$$

This neutral species has only been observed at total vanadium concentrations of 0.0001 M or less.[27]

For both samples A and B, the resulting gel was initially brown, but within hours the color turned dark red. Work done by Pozarnsky and McCormick[4,5] on the condensation of an acidified metavanadate solution discussed several possible routes of $[V^{5+}O_2]^+ \rightarrow$ polymer. Using ESR, they reported detecting small amounts of $[V^{4+}O]^{2+}$. Although present at very low concentrations (~0.001 M), they proposed that the dimerization of the $[V^{(5+)}O_2]^+$ and $[V^{4+}O]^{2+}$ to form a mixed valence species might initiate polymerization.[28] However, their experiments utilized an ion-exchange column, which according to their report,[4] was the source of the V^{4+} needed to initiate this dimerization. In the current work, an ion-exchange column was not utilized, but a similar polymerization process likely occurred. Since V^{4+} cannot be observed using the NMR techniques used in this work and since the total concentration of vanadium in solution remained constant until polymerization began, the amount of V^{4+} present is very small. If V^{4+} existed during our preparations, the source might be attributed to the following: (1) the reduction of the dioxovanadate cation (observed in acidic media[29])

$$[V^{(5+)}O_2]^+ + 2H^+ + e^- \rightarrow H_2O + [V^{(4+)}O]^{2+}$$

and/or (2) the reduction of V^{5+} to V^{4+} with O_2^- to form a $V^{4+}-OO$ moiety. This reaction has also been reported in the literature.[30]

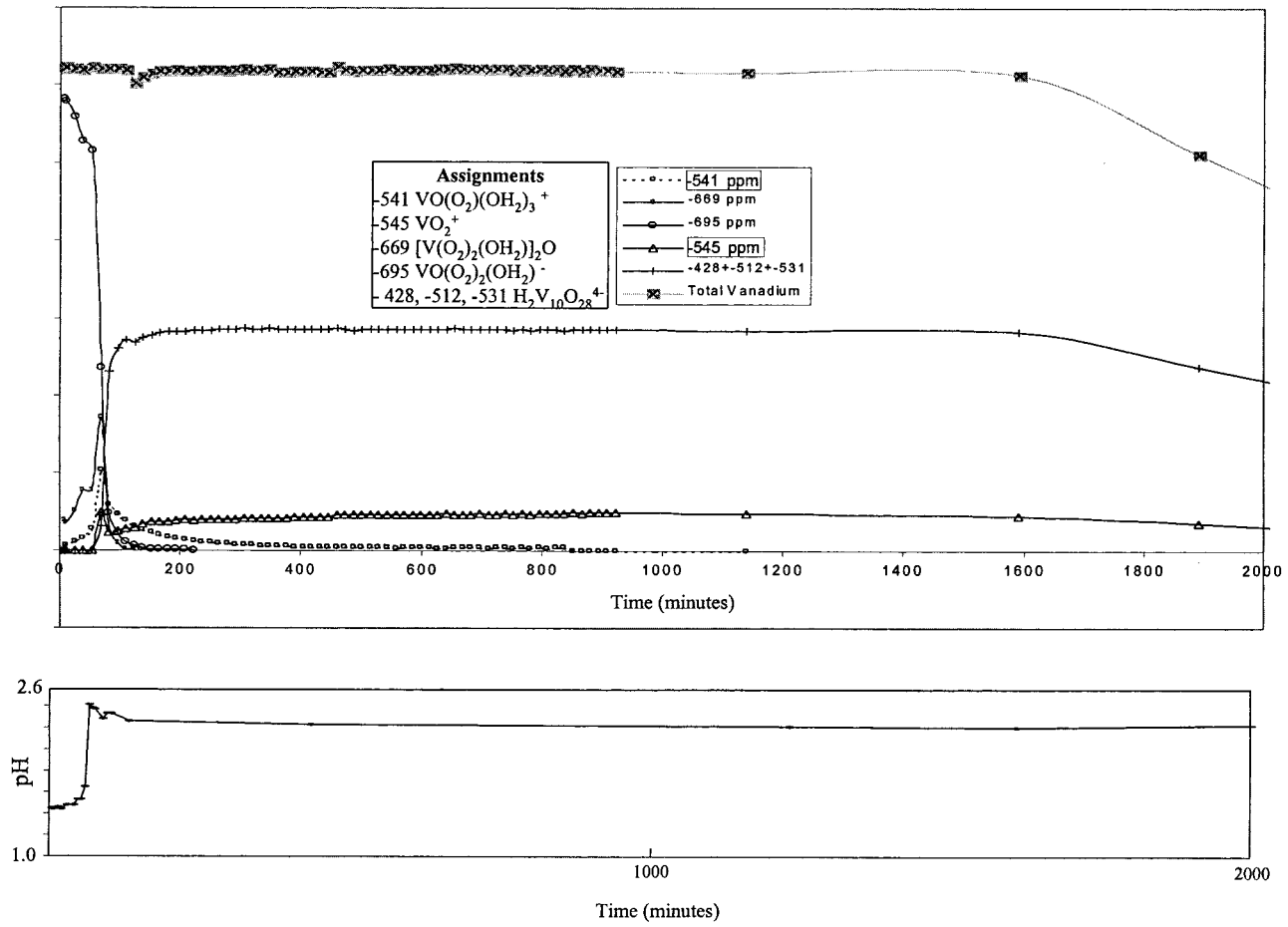

Figure 13. ^{51}V solution NMR vs time and pH vs time of sample B.

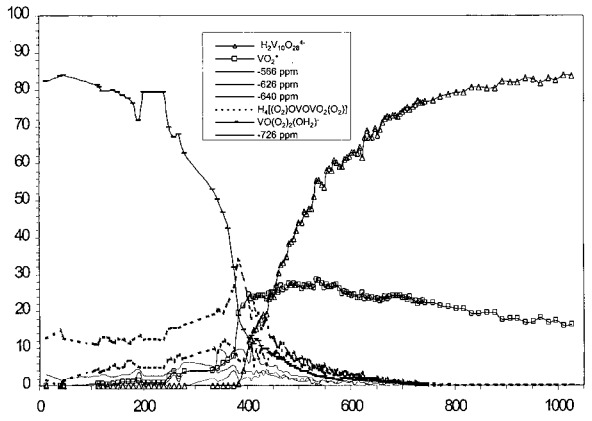

Figure 14. ^{51}V NMR vs time for sample C (normalized to total vanadium in solution).

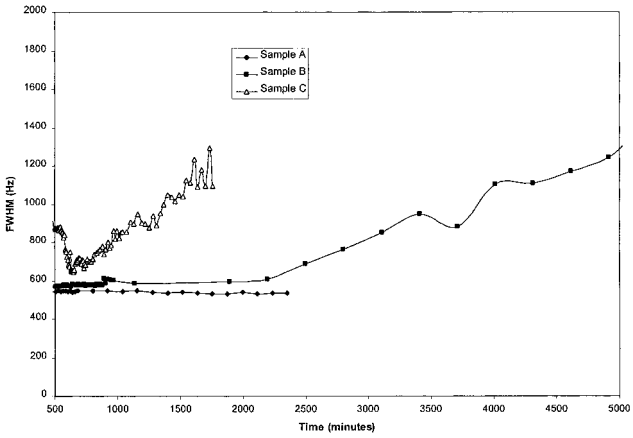

Figure 15. ^{51}V NMR peak width broadening of the VO_2^+ peak in (a) sample A, (b) sample B, and (c) sample C.

We did not observe any polymerization in samples A and B until all of the peroxovanadates had decomposed. For sample A, this occurred at about 1400 min and in sample B at about 1600 min. Since H_2O_2 has been reported[30] to oxidize V^{4+} to V^{5+}, it is conceivable that the monoperoxovanadate cation oxidized the available V^{4+}, effectively scavenging the proposed initiator and stopping polymerization. Polymerization began either at exactly the same time or immediately after the monoperoxovandate cation had entirely disappeared. Other authors have reported that V^{4+} can be considered a polymerization initiator.[30,31] In sample C, gelation began much sooner at about 600 min (Figure 14), even though the temperature was much lower. Gelation began and proceeded in the presence of several peroxovanadates, some of which are still unidentified. It was not clear whether these were involved in gel formation or were simply trapped since by 1000 min the entire liquid volume and the remaining species in solution were contained within the solid matrix. The resulting material was initially green, but within hours it had turned dark brown. Other research indicated that the gel may have more than 20% of the vanadium present as V^{4+}.[32] This amount of V^{4+} was unlikely since ^{51}V relaxation times were measured and were similar for each sample. Previous literature indicates that about 1% of the vanadium is present as V^{4+}.[31]

As the polymerization proceeded, broadening of the VO_2^+ peak was observed for samples B and C, but not in A (Figure 15). In sample B, the full width at half-maximum (fwhm) of

this peak increased from a value of 493 Hz at $t = 31.5$ h to a value of 1333 Hz at $t = 87$ h. The broadening of this peak in sample C was even greater, as it was observed to increase from 620 Hz at 600 min to 1200 Hz at 1800 min. Pozarnsky and McCormick[4] observed some broadening of this peak, although to a much lesser extent. Most likely, this broadening is associated with the reduced mobility of ^{51}V nuclei in polymeric chains. The interaction of observable V^{5+} with paramagnetic V^{4+} may cause additional broadening.

Although similar precursors were apparently involved in the gelation, the ^{51}V NMR spectra of the resulting vanadia gels were different than those previously reported.[4,21] The gels prepared by our methods (both wet and ambiently dried) have four distinct vanadium nuclei, not one as previously reported.

5. Conclusions

Peroxovanadate dimers have been shown to be involved in the η^2-peroxo ligand decomposition. These dimers were present only in excess H_2O_2 and were fairly unstable; nevertheless, they were present in appreciable amounts. These species could be identified by previously unreported Raman bands. The bands at 960, 910, and 600 cm^{-1} were assigned to a symmetrical neutral dimer, $[V(O_2)_2]_2O(OH_2)_2$. This species was only present at lower pH and in the presence of the diperoxovanadate anion with excess H_2O_2. An asymmetrical dimer ($H_4[(OO)_2OVOVO_2$-$(OO)]$) had Raman bands at 955, 910, and 599 cm^{-1} with an additional broad feature between 500 and 400 cm^{-1}. Both dimers were important intermediates in the sol−gel chemistry.

The peroxovanadates present at the lower H_2O_2/V ratio and lower vanadium concentration decomposed before gelation began, leaving a solution containing the diprotonated decavanadate ion and the dioxovanadate cation. Gelation proceeded via the same precursors as previously reported by other authors, although the ^{51}V 10 kHz MAS spectrum of the wet gel indicated that the final gels were different. It has been recently reported[6] that the addition of excess H_2O_2 to these peroxovanadate solutions only slows the condensation process and does not lead to a new form of V_2O_5 gel. Our results indicate that at these lower H_2O_2 and vanadium concentrations, the addition of excess H_2O_2 increases the duration of the diperoxovanadate stability. This effectively delays the onset of condensation. But once the excess H_2O_2 has been consumed, condensation is completed much sooner.

At higher H_2O_2/V ratios and higher vanadium concentrations, gelation began sooner, at much lower temperatures, and in the presence of several peroxovanadates. When gelation was complete, the aqueous solution initially present was entirely contained within the final solid gel.

Acknowledgment. The authors would especially like to thank Dr. R. E. McCarley of the Department of Chemistry and the Ames Laboratory−USDOE for helpful discussions. This work was conducted with support from the Ames Laboratory−USDOE under Grant No. W-7405-Eng-82.

References and Notes

(1) Kudo, T.; Okamoto, H.; Matsumotot, K.; Sasaki, Y. *Inorg. Chim. Acta* **1986**, *111*, L27.
(2) Aakoi, A.; Nogami, G. *J. Electrochem. Soc.* **1996**, *143*, L191.
(3) Hinokuma, K.; Ogasawara, K.; Kishimoto, A.; Kudo, T. *Solid State Ionics* **1992**, *507*, 53.
(4) Pozarnsky, G. A.; McCormick, A. V. *Chem. Mater.* **1994**, *6*, 380.
(5) Pozarnsky, G. A.; McCormick, A. V. *J. Mater. Chem.* **1994**, *4* (11), 1749.
(6) Alonso, B.; Livage, J. *J. Solid State Chem.* **1999**, *148*, 16.
(7) Fontenot, C. J.; Wiench, J. W.; Pruski, M.; Schrader, G. L. *J. Phys. Chem.*, submitted for publication.
(8) Schroeder, W. D.; Fontenot, C. J.; Schrader, G. L. Manuscript in preparation.
(9) Brazdil, J. F.; Toft, M. A.; Bartek, J. P.; Teller, R. G.; Cyngier, R. M. *Chem. Mater.* **1998**, *10*, 4100.
(10) Brazdil, J. F. *CHEMTECH* **1999**, *29*, 1, 23.
(11) Toft, M. A.; Brazdil, J. F., Jr.; Glaeser, L. C. U.S. Patent 4784979, 1988.
(12) Schwendt, P.; Pisarcik, M. *Spectrochim. Acta A* **1990**, *46A* (3), 397.
(13) Campbell, N. J.; Dengel, A. C.; Griffith, W. P. *Polyhedron* **1989**, *8* (11), 1379.
(14) Griffith, W. P.; Lesniak, P. J. *J. Chem. Soc. A* **1969**, *7*, 1066.
(15) Schwendt, P.; Volka, K.; Suchanek, M. *Spectrochim. Acta A* **1988**, *44A* (8), 839.
(16) Howarth, O. W.; Hunt, J. R. *J. Chem. Soc., Dalton Trans.* **1979**, 9, 1388.
(17) Conte, V.; Di Furia, F.; Moro, S. *J. Mol. Catal. A: Chem.* **1997**, *120* (1−3), 93.
(18) Harrison, A. T.; Howarth, O. W. *J. Chem. Soc., Dalton Trans*. **1985**, 6, 1173.
(19) Jaswal, J. S.; Tracey, A. L. *Inorg. Chem.* **1991**, *30*, 3718.
(20) Shinohara, N.; Nakamura, Y. *Bull. Chem. Soc. Jpn.* **1989**, *62* (3), 734.
(21) Fontenot, C. J.; Wiench, J. W.; Pruski, M.; Schrader, G. L. To be submitted for publication.
(22) Conte, V.; Furia, F.; Moro, S. *J. Mol. Catal. A* **1997**, *117*, 139.
(23) Schwendt, P.; Pisarcik, M. *Chem. Pap.* **1988**, *42* (3), 305.
(24) Schwendt, P. *Collect. Czech. Chem. Commun.* **1983**, *48*, *8* (1), 248.
(25) Butler, A.; Clague, M. J.; Meister, G. E. *Chem. Rev.* **1994**, *94*, 625.
(26) Livage, J.; Henry, M.; Sanchez, C. *Prog. Solid State Chem.* **1988**, *18* (4), 259.
(27) Baes, C.; Mesmer, R. *The Hydrolysis of Cations*; John Wiley and Sons: New York. 1976; Chapter 10.
(28) Rodriguez, R. *Principles of Polymeric Systems*; John Wiley and Sons: New York, 1988.
(29) Latimer, W. M. *Oxidation Potentials*, 2nd ed.; Prentice-Hall: New York, 1952.
(30) Liochev, S.; Fridovich, I. *Arch. Biochem. Biophy.* **1991**, *291*, 2, 379.
(31) Gharbi, N.; Sanchez, C.; Livage, J.; Lemerle, J.; Nejem, L.; Lefebvre, J. *J. Inorg. Chem.* **1982**, *21*, 2758.
(32) Sanchez, C., Navavi, M., Tauelle, F. *Mater. Res. Soc. Symp. Proc.* **1988**, *121*, 93.
(33) Griffith, W. P.; Wickins, T. D. *J. Chem. Soc. A* **1966**, 1087.